Increasing the Lifetime of Boeing Employees, by Decreasing Fatigue

MEC E 563 — University of Alberta

Jacob Zimmel, Brandon Martens, Abdalla Babikir, Douglas O'Brien, Wesley Eze
Student IDs: 1660615, 1632471, 1658307, 1687801, 1672318
March 8, 2025

Table of Contents

List of Figures

1 Abstract

This study investigates how fuel placement and quantity affect the loading of a Boeing 747-8 aircraft under steady flight. Finite Element Method (FEM) is utilized to determine the optimal positions of wing fuel.

2 Introduction

Commercial aircraft store fuel in wings for safety, engine proximity, and structural rigidity [1]. This study investigates how fuel storage in Boeing 747-8 wings reduces root stress, extends fatigue life, and identifies optimal fuel placement to minimize wing loading. A static structural finite element model (FEM) was developed in ANSYS Workbench using a quadrilateral mesh of shell elements. The wing was modeled as a hollow shell with uniform thickness adjusted to approximate the moment of inertia of a stiffened wing structure.

Fuel constitutes up to 44% of the aircraft's maximum weight [2], making its placement critical for performance. Two loading conditions were analyzed:

- **Lift**: Elliptical pressure distribution based on Prandtl's lifting-line theory.
- **Fuel weight**: Uniform pressure on the wing's lower face (inboard, outboard, and reserve tanks; Figure 1).

Thrust effects were neglected due to the wing's high stiffness in the thrust direction, and engine weight (less than 7% of total mass [3]) was excluded. The simplified shell model prioritized computational efficiency over localized accuracy, with trade-offs including:

- **Benefits**: Reduced computational cost via plane stress simplification; practical meshing for thin structures.
- **Challenges**: Uniform thickness assumption; simplified geometry at critical regions (e.g., wing root, engine mounts); limited rivet/bolt modeling.

While absolute stress values require refinement, the model provides insights into fuel placement effects. This study aims to:

1. Analyze wing response to lift and fuel loads.
2. Quantify fatigue life improvements from wing fuel storage.
3. Identify optimal mid-flight fuel placement.
4. Validate the shell model against analytical and real-world data.

3 Methodology

3.1 Assumptions

The following assumptions are made to simplify the structural and aerodynamic analysis of the aircraft wing:

- The entire wing is composed of Aluminum 7075-T6, a common aerospace material.
- No internal structural components such as spars or ribs are included in the finite element analysis (FEA) model.
- The wing shape is approximated as an elliptical cross-section to better match real aircraft lift distribution.
- The wing is treated as a cantilever beam, fixed at the root, with a tapered cross-section.
- An elliptical lift distribution is applied to model how lift varies along the wing span.

3.2 Given Data

$$\begin{aligned}
L &= 39.0\text{ m, wing span [4]}\\
c_{\text{root}} &= 14.654\text{ m, root chord [5]}\\
c_{\text{tip}} &= 0.982\text{ m, tip chord [5]}\\
h_{\text{root}} &= 1.6\text{ m, root height [5]}\\
h_{\text{tip}} &= 0.1\text{ m, tip height [5]}\\
t &= 0.023\text{ m, wall thickness}\\
E &= 71.7\text{ GPa, Young's modulus for 7075-T6 [6]}\\
\sigma_y &= 503\text{ MPa, yield strength of 7075-T6 [6]}\\
w_0 &= \frac{2\times(440000\times 9.81)}{\pi\times L} \quad \text{[Distributed load (N/m)] [4]}
\end{aligned}$$

where:

- w_0: Distributed load - Load distribution across the wing span (N/m) [4]

3.3 Simplified Governing Equations for Analysis

The airfoil geometry is simplified to an elliptical profile, with the outer and inner radii defined as:

$$a_{\text{outer}}(x) = \frac{c_{\text{root}}}{2}\left(1-\frac{x}{L}\right) + \frac{c_{\text{tip}}}{2}\frac{x}{L}$$

$$b_{\text{outer}}(x) = \frac{h_{\text{root}}}{2}\left(1-\frac{x}{L}\right) + \frac{h_{\text{tip}}}{2}\frac{x}{L}$$

The moment of inertia for a hollow ellipse is:

$$I_x(x) = \frac{\pi}{4}\left(a_{\text{outer}}b_{\text{outer}}^3 - a_{\text{inner}}b_{\text{inner}}^3\right)$$

The distributed load varies along the span as:

$$w(x) = w_{\text{root}}\sqrt{1-\left(\frac{x}{L}\right)^2}$$

For deflection, the governing equation is:

$$\frac{d^2}{dx^2}\left(EI(x)\frac{d^2v}{dx^2}\right) = w(x)$$

with boundary conditions:

$$v(0)=0, \quad \frac{dv}{dx}(0)=0, \quad \frac{d^2v}{dx^2}(L)=0, \quad \frac{d^3v}{dx^3}(L)=0$$

The deflection is solved numerically due to the complex terms involved. The full derivation and calculation of the deflection can be found in Appendix A.

3.4 Simulation Setup

The computational domain and boundary conditions are shown in Figure 1. The wing root was fixed as a cantilever beam, with variable loading conditions. Two steady flight cases were analyzed with elliptical lift distributions:

- **Full fuel**: $L(x) = 5.05\text{kPa}\sqrt{1 - x^2/39^2}$
- **Half fuel**: $L(x) = 3.95\text{kPa}\sqrt{1 - x^2/39^2}$

Fuel distribution followed a representative estimate obtained from the FEA [7] where: inboard (52%, 50.6 tonnes), outboard (19%, 18.2 tonnes), and reserve (2%, 2.0 tonnes) fuel tanks capacities and locations were provided. Pressure loads were applied to tank locations using gravity loading and surface area calculations.

With the full fuel load, two cases were analyzed to determine the stress difference between flying with fuel in the wings vs. all the fuel in the fuselage. With these stress values the number of cycles could be calculated to figure out the difference in lifetime.

The half-fuel case looked at determining the stress and deflection to determine which configuration would be better for mid-flight turbulence and maneuvers. Two half-fuel scenarios are:

- Case A: Primarily empty inboard tank
- Case B: Empty outboard/reserve tanks

A 2D shell mesh with applied thickness was used, calibrated to achieve 4m tip deflection in the full fuel case as seen in figure 2. Convergence criteria were tightened from 5% to 0.25% after initial iterations, requiring four total iterations for solution stability, as seen in figure 3.

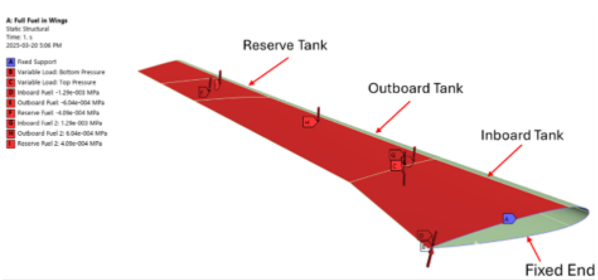

Figure 1: Schematic of the computational domain (not to scale)

4 Verification and Validation

A quadrilateral mesh was selected for superior metrics (skewness ≈ 0, aspect ratio ≈ 1) compared to triangular elements. Initial first-order shell elements (1,335 nodes) were adaptively refined to 17,552 nodes in high-stress regions (Figure 2).

Figure 2: Converged mesh of wing structure

A convergence study for the full-fuel case (Figure 3) showed solution stabilization at 3.93m tip deflection, confirming mesh independence. Verification against analytical results (1.7m deflection) revealed order-of-magnitude agreement, with discrepancies attributed to the analytical model's simplified hollow elliptical geometry.

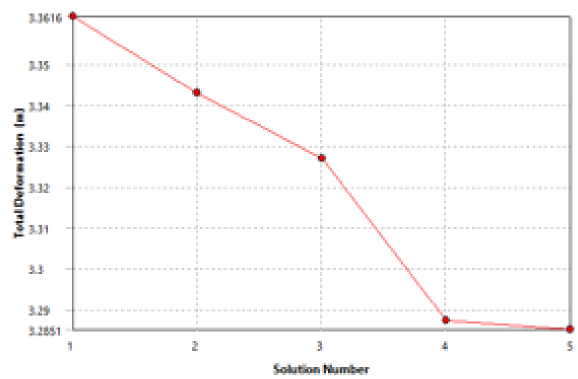

Figure 3: Tip deflection vs mesh refinement

Validation against real-world data showed consistency with:

- Airbus A380-800 deflection (4m at 39.9m span) [8]
- Industry-standard 10-15% wingtip deflection [9]

The simulated 3.93m deflection (10.1% of 39m span) confirms model reliability.

5 Results & Discussion

The first case investigates the wing loaded with full fuel tanks. In this case, the fuel weight partially counteracts the lift-induced pressure load, reducing the net load on the wing. Non-physical stress concentrations were observed at locations where the airfoil's height changes abruptly; these were neglected. The maximum physical stress was found to be 177 MPa, and the maximum wingtip deflection was 3.93 m. See Figure 4 for the Von Mises stress contour. This case best represents the actual loading condition of a Boeing 747 wing. For instance, the Airbus A380-800 (wingspan 79.8 m) shows over 4 m deflection [8], and the Boeing 747-8 (wingspan 78 m [3]) is expected to behave similarly.

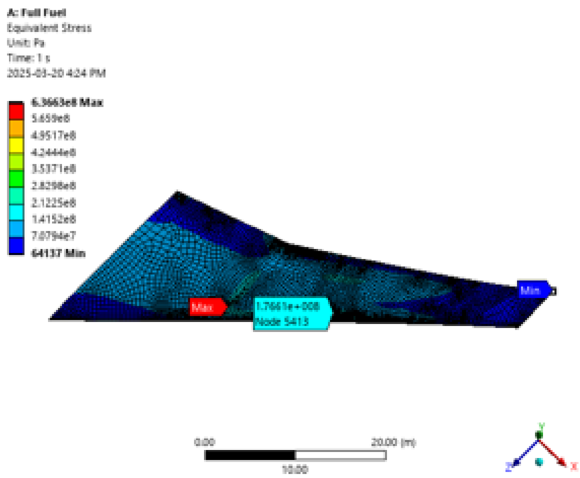

Figure 4: Max Lift with Full Fuel in Tanks

The second case applies the same lift forces without the fuel weight in the wing (Figure 5). In this scenario, a larger maximum stress of 200 MPa and a deflection of 4.31 m were observed. Non-physical stress peaks were again neglected.

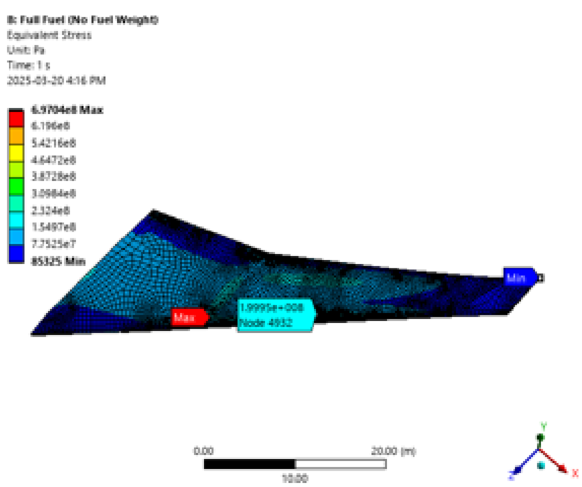

Figure 5: Max Lift with No Fuel in the Tanks

Comparing these two cases indicates that internal fuel storage reduces maximum stress and deflection, which in turn increases fatigue life. Figure 6 illustrates that the lower maximum stress due to fuel weight increased fatigue life by 300,000 cycles—from 200,000 to 500,000 cycles. Although actual Boeing 747s complete around 20,000 flights [10], the discrepancy is attributable to turbulence and maneuvering, which cause multiple loading cycles per flight.

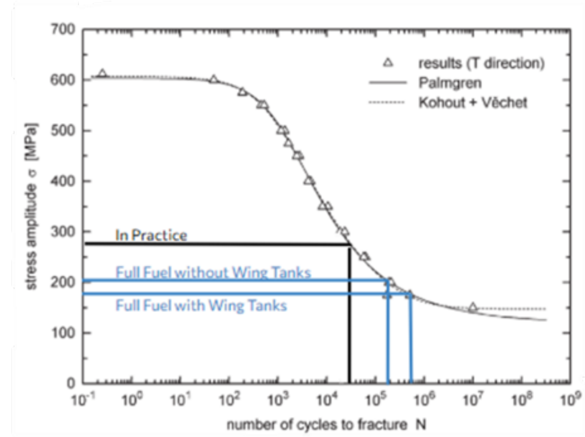

Figure 6: Fatigue Life Improvement with In-Wing Fuel

To quantify the impact of fuel distribution on wing loading, two optimized placement strategies were analyzed under half-fuel conditions (50% capacity):

- **Inboard storage**: Fuel concentrated near the fuselage (Figure 7) resulted in 2.57m tip deflection. This configuration creates shorter moment arms for fuel weight forces, reducing their effectiveness in counteracting lift-induced bending.
- **Outboard storage**: Distributing fuel toward wingtip tanks (Figure 8) decreased deflection by 16% to 2.16m. The increased moment arm (∼78% of wingspan vs 32% for inboard) provides greater mechanical advantage against lift forces, demonstrated by:
  - 19% lower peak stress (157 MPa vs 194 MPa)
  - More uniform stress distribution along wing spar

The 0.41m deflection reduction demonstrates that strategic fuel placement near anti-nodes (wingtip tanks) significantly improves load distribution - critical for fatigue life enhancement during turbulent flight conditions where stress cycles accumulate rapidly.

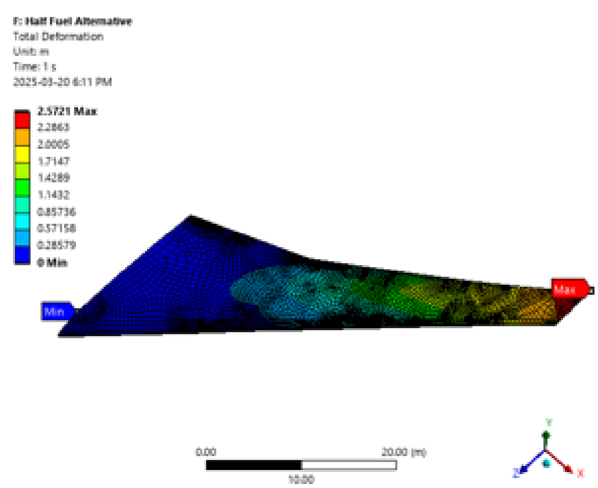

Figure 7: Deflection with Fuel Stored in Inboard Tanks

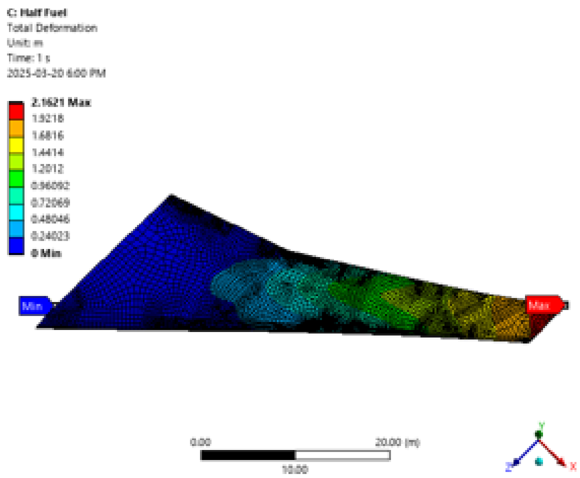

Figure 8: Deflection with Fuel Stored near Wing Tip

The case with fuel placed near the wingtip exhibits a 17% lower deflection and 19% lower maximum stress than the inboard fuel case. This is consistent with the expectation that fuel weight applied further from the wing root provides a greater moment to counteract lift, thus reducing stress and enhancing fatigue life.

All simulations revealed non-physical stress spikes at the junction between inboard and outboard sections due to abrupt geometry changes; these spikes were omitted in reporting the maximum stress. Additionally, a bubbling deformation was observed in the shell model—a consequence of modeling the wing as a uniform, thickened shell rather than including internal stiffeners. Although this produces a slight visual artifact, the overall wing stiffness remains comparable to that of the actual structure.

The deflection results for the full-fuel case align well with experimental and reported aircraft data [8, 9], confirming that the simulation outputs are physical. Comparisons with the analytical model, which predicted a deflection of 1.7 m and a maximum stress of 115 MPa, show discrepancies attributed to the simplifying assumptions (e.g., elliptical cross-section and linear tapering) used in the analytical approach.

Overall, these results highlight the impact of fuel placement on wing performance and provide insight into the limitations and accuracy of both the FEM and analytical models.

6 Conclusion

This study has achieved its main objectives:

1. Analyze the wing response to lift and fuel loads.
2. Quantify fatigue life improvements from wing fuel storage.
3. Identify optimal mid-flight fuel placement.
4. Validate the shell model against analytical and real-world data.

These objectives were addressed through two analyses: (1) storing fuel in the wings and (2) storing fuel near the wingtips.

The primary conclusion is that fuel placement significantly impacts an aircraft's lifespan. Storing fuel in the wings reduced the worst-case steady flight load from 200 MPa to 177 MPa, resulting in an increase of 300,000 cycles in fatigue life. This demonstrates that even a modest reduction in stress can substantially extend the aircraft's lifetime.

Furthermore, placing fuel closer to the wingtip lowered in-flight stresses by 19%. This reduction is critical because turbulent loads can cause stress spikes that might lead to wing failure; a lower baseline stress helps keep these spikes minimal, thereby improving durability.

The study also revealed that while an analytical solver offers a valuable benchmark, it struggles with the real wing's complex geometry—particularly with the airfoil shape and abrupt slope transitions. Empirical industry data was essential for validating deflection and stress estimates, which, in turn, confirmed the physicality of the simulation results.

Overall, the FEM model successfully approximated the bending loads due to lift and fuel, with the fixed wing root connection reasonably representing the actual attachment. However, improvements such as incorporating internal structures to reduce non-physical bubbling and refining the model to better capture sharp geometry transitions are recommended for future work. These enhancements would further elucidate the influence of fuel placement on wing fatigue life and overall performance.

While this model does not account for all the complexities of aircraft fuel management, it clearly demonstrates its importance. By completing our objectives, we have shown that fuel placement and management are integral to the design of a successful aircraft.

7 Appendix A: Analytical Approach to Wing Analysis

7.1 Geometry of a Hollow Ellipse

The 747's airfoil geometry is highly complex due to winglets, flaps, spoilers, and ailerons, making analytical modeling impractical. To simplify, the wing cross-section is approximated as an ellipse that tapers along the span. This section outlines the analytical modeling approach used to compare with FEA results.

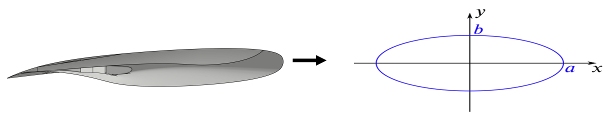

Figure 9: Simplification of the plane wing from complex geometry to ellipse

The cross-section of a 1:1 model of the 747-8 Freighter was taken to obtain the dimensions of the wing that were used to approximate the ellipse shape.

$$\begin{aligned} a_{\text{outer}}(x) &= \frac{c_{\text{root}}}{2}\left(1-\frac{x}{L}\right)+\frac{c_{\text{tip}}}{2}\frac{x}{L} \\ b_{\text{outer}}(x) &= \frac{h_{\text{root}}}{2}\left(1-\frac{x}{L}\right)+\frac{h_{\text{tip}}}{2}\frac{x}{L} \\ a_{\text{inner}}(x) &= a_{\text{outer}}(x)-t \\ b_{\text{inner}}(x) &= b_{\text{outer}}(x)-t \\ I_x &= \frac{\pi}{4}(a_{\text{outer}}\,b_{\text{outer}}^3-a_{\text{inner}}\,b_{\text{inner}}^3) \end{aligned}$$

7.2 Distributed Load (Elliptical Profile)

Plane wings take on an elliptical distribution of force from the root of the wing to the tip of the wing, decreasing accordingly. The assumption used to determine that distributed force is that the plane wing would handle half the weight of the plane.

$$w(x) = w_{\text{root}}\sqrt{1-\left(\frac{x}{L}\right)^2}, \quad w(0)=w_{\text{root}}, \quad w(L)=0$$

$$w_{\text{root}} = \frac{2W_{\text{plane}}}{\pi L}$$

$$w(x) = \frac{2W_{\text{plane}}}{\pi L}\sqrt{1-\left(\frac{x}{L}\right)^2}$$

7.3 Bending Moment

$$\begin{aligned} M(x) &= \int_x^L w(\eta)(\eta-x)\,d\eta \\ &= w_{\text{root}}L^2\int_{x/L}^1 \sqrt{1-u^2}\left(u-\frac{x}{L}\right)du \end{aligned}$$

7.4 Bending Stress

$$\sigma(x) = \frac{M(x)\,b_{\text{outer}}(x)}{I(x)}$$

7.5 Deflection

$$\frac{d^2}{dx^2}\left(EI(x)\frac{d^2v}{dx^2}\right) = w(x)$$

Boundary Conditions:

$$v(0)=0, \quad \frac{dv}{dx}(0)=0, \quad \frac{d^2v}{dx^2}(L)=0, \quad \frac{d^3v}{dx^3}(L)=0$$

The final integral for the deflection requires numerical integration, which has been done through the use of Python.

7.6 Python Code Results

The python code generated the following figures and results that were used to conduct the FEA analysis:

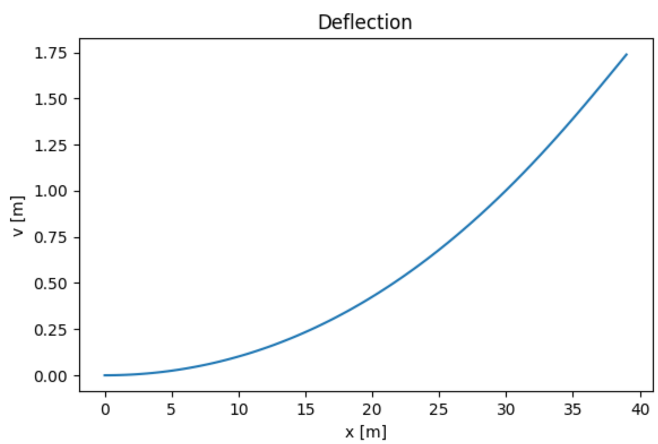

Figure 10: Produced figures from Python Code — 1

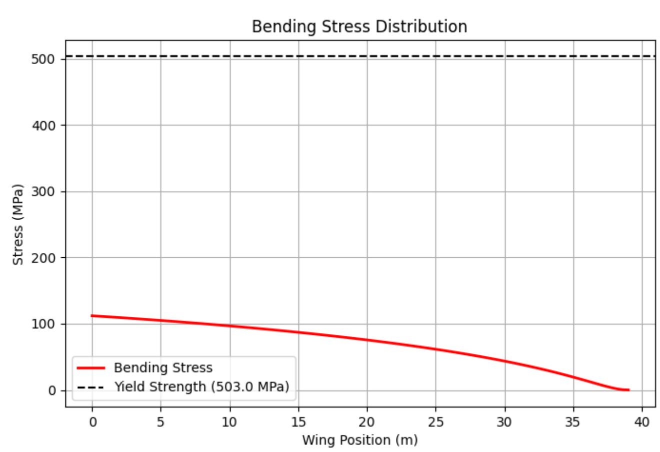

Figure 11: Produced figures from Python Code — 2

References

[1] A. Tompkins. (2021) This is why fuel tanks are located in aircraft wings. Accessed: 2025-03-20. [Online]. Available: https://airplaneacademy.com/this-is-why-fuel-tanks-are-located-in-aircraft-wings/

[2] M. Kingsley-Jones. (2012) In focus: Boeing 747-8 technical description and cutaway. Accessed: 2025-03-10. [Online]. Available: https://www.flightglobal.com/in-focus-boeing-747-8-technical-description-and-cutaway/107801.article

[3] ——. (2012, Mar.) In focus: Boeing 747-8 technical description and cutaway. Accessed: 10-Mar-2025. [Online]. Available: https://www.flightglobal.com/in-focus-boeing-747-8-technical-description-and-cutaway/107801.article

[4] FlightGlobal, "In focus: Boeing 747-8 technical description & cutaway," *FlightGlobal*, 2011, accessed: 2025-03-21. [Online]. Available: https://www.flightglobal.com/in-focus-boeing-747-8-technical-description-and-cutaway/107801.article

[5] GrabCAD, "Boeing 747-8 freighter," n.d., accessed: 2025-03-21. [Online]. Available: https://cad.grabcad.com/library/boeing-747-8-freighter-1

[6] A. International, "Aluminum alloy 7075-t6," n.d., accessed: 2025-03-21. [Online]. Available: https://asm.matweb.com/search/specificmaterial.asp?bassnum=ma7075t6

[7] FAA. (2022, Dec.) Boeing 747-100, trans world airways flight 800, n93119. Accessed: 26-Mar-2025. [Online]. Available: https://www.faa.gov/sites/faa.gov/files/images/lessons_learned/N93119/tanks_capacities.jpg

[8] British Airways. (2025) Airbus a380-800. Accessed: 3-Apr-2025. [Online]. Available: https://www.britishairways.com/content/information/about-ba/fleet-facts/airbus-a380-800

[9] DLR. (2020) Bending instead of snapping. Accessed: 3-Apr-2025. [Online]. Available: https://elib.dlr.de/140326/1/2020_dlrmagazin-166-bending-instead-of-snapping.pdf

[10] M. M. Spencer. (1972) The boeing 747 fatigue integrity program. Accessed: 15-Mar-2025. [Online]. Available: https://ntrs.nasa.gov/api/citations/19720022248/downloads/19720022248.pdf